Journal of Analytical and Applied Pyrolysis 189 (2025) 107064

Contents lists available at ScienceDirect

Journal of Analytical and Applied Pyrolysis

journal homepage: www.elsevier.com/locate/jaap

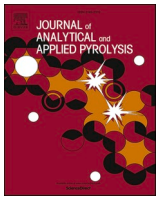

Co-activation of Martian regolith and hydrochar for enhanced water retention and water holding capacity

Robert W. Cheatham, Al Ibtida Sultana, M. Toufiq Reza *

Department of Chemistry and Chemical Engineering, Florida Institute of Technology, 150 West University Boulevard, Melbourne, FL 32901, USA

ARTICLE INFO

Keywords:
Activation
Biochar
Hydrochar
Martian regolith
Water holding capacity
Water retention

ABSTRACT

With the goal of sustainable life on Mars, the importance of maximizing the use of all available materials has become crucial. One such method in which to utilize the available resources is through the synthesis of a carbon-rich, porous material, creating a material fit for a variety of essential applications such as water retention. This study improved the water retention properties of Martian regolith through co-activation with pine, a carbon-rich biomass. To enhance carbon porosity, biomass was first hydrothermally carbonized at 260°C, and combined with Martian regolith (0, 5, 10, 25, 50 % w/w) before being chemically co-activated using potassium hydroxide as an activation agent, for two hours, at 800 °C. The co-activated regolith samples were characterized to quantify surface porosity, morphology appearance analysis by scanning electron microscopy, crystallinity analysis by powder X-ray diffraction, and chemical composition analyses by proximate and ultimate analyses. The results highlight an increased surface porosity of 287 %, with a 50 % addition of hydrochar, and minimized water loss from 24 % to just 4 % as well as an increased water holding capacity of 16 % with an increase in Martian regolith from 50 % to 95 %.

1. Introduction

Long-term human space missions to Mars have generated the need for resources to support the inhabitancy, which has become crucial. Energy, oxygen, construction materials, water, and food are the top five commodities required for human civilization settlement on Mars [1]. On the surface of the planet Mars, the first four are abundant in economically viable concentrations and in forms that can be extracted. For example, solar energy can probably be supplemented by nuclear fission reactors; water, which can be found in hydrated minerals and ice; oxygen, which can be extracted from atmospheric CO_2; and building materials, such as bricks and other derivatives can be processed from Martian regolith [2]. However, naturally occurring sources of food are non-existent in Mars and the capability of producing food, using the natural resources available is hampered by the characteristics of Martian regolith such as poor water retention and low carbon content [3,4].

Literature also discussed the potential of Martian regolith and its importance for sustaining life, while also revealing the challenges of utilizing Martian regolith. Wamelink *et al.* discussed the difficulties of maintaining water in pure regolith samples, reporting pure regolith has a low water holding capacity of about 30 % and Earth's natural soil was attributed to have 100 % water holding capacity while also mentioning the need for the remediation of the moisture retention capabilities of Mars regolith [5]. This can be accounted for by the fact that Martian regolith is primarily composed of weathered mafic rock [4,6]. As a result, water seeps away, decreasing the effective use of the already limited amount of water available, similar to the interaction between sand and water here on Earth [7]. To amend this, Jänchen *et al.* sought to utilize microorganisms as a method of amending the water retention properties of regolith but were found to remove water from the Mars regolith [8]. Instead of focusing on microorganisms, other studies tackling corollary challenges on planet Earth, successfully highlighted the importance of improving a soil's moisture retention capacity, which is a key factor in applications such as crop growth, by the addition of carbon-dense solids. Caporale *et al.* attempted to combined compost with Martian regolith and reported favorable soil amendment results but attributed the water retention capabilities to the compost while the water retention capabilities of the Martian regolith remained constant [9]. This method requires large amounts of compost to be added frequently, which in applications such as space travel, is not efficient due to the limited room on shuttles [2]. This also does not alter the existing properties of Martian regolith but rather relies on the properties

* Corresponding author.
E-mail address: treza@fit.edu (M.T. Reza).

https://doi.org/10.1016/j.jaap.2025.107064
Received 30 December 2024; Received in revised form 7 February 2025; Accepted 27 February 2025
Available online 28 February 2025

of the compost to offset those of the Martian regolith, leaving the sustainability and efficiency of this method in question.

In this study, biochar was chosen as the carbon rich solid in which to amend the properties of Martian Regolith. Literature demonstrated that the addition of biochar, here on earth, significantly improves the water-holding capacity of the soil, increasing the water available to plants, due to the increased pore volume and total porosity of char-amended soil [10]. Surface morphology (total pore volume, specific surface area, pore structure) and surface chemistry (functional groups present) of the char-amended soil also positively affect the water absorption rate [11]. Moreover, the addition of char has been previously reported to improve physical characteristics, such as bulk density, which improves the softness and terrene of the char-amended soil [12], promoting crop yield. For example, the addition of carbon-dense biochar to sandy loam soil was demonstrated to reduce bulk density by 6.3 % and improve water holding capacity by 9 %, with the addition of about 17 kg of biochar for every cubic meter of sand, owing to biochar's surface porosity characteristics [13]. In another study, biochar was utilized for soil amendment, enhancing soil properties such as porosity, resulting in an increase in the total porosity of the amended soil by an average of 52.7 % and hence increase in moisture content, of the char-amended soil, by 5.33 % [10]. Garbowski *et al.* also emphasized the impact biochar can have on the carbon content with biochar having 11.1 % more grams of carbon per kg of soil [14].

Therefore, this study focuses on investigating the properties of Martain regolith and thermally treated hydrochar. Moreover, the properties of Martian regolith were sought to be improved through coactivation with hydrochar, to form a novel material. Hydrochar was formed via the utilization of hydrothermal carbonized (HTC) loblolly pine, a thoroughly researched biomass, a material known for its favorable porosity and carbon content [15,16]. This enabled co-activated Martian regolith-hydrochar material to be tailored for beneficial extra-terrestrial applications such as water retention and water holding capacity (WHC). This maximizes the positive characteristics of the existing Martian regolith, thus emulating a practical solution for increasing resource utilization on Mars.

2. Materials and methodology

2.1. Materials

Loblolly Pine (LP) was obtained from Idaho National Laboratory (ID, USA) with a particle range of 149–595 μm. Mars global simulant Martian regolith (MR), made to emulate real Martian rock found in the Gale crater, on planet Mars, was purchased from Space Resource Technologies (Orlando, FL, USA) and had a particle size ranging from less than 0.04–100 μm. Potassium hydroxide (KOH), 2 N hydrochloric acid (HCl), and 0.01 N sodium hydroxide (NaOH) were obtained from Fisher Scientific (Fair Lawn, NJ, USA).

2.2. Mars regolith-activated hydrochar composite preparation

LP underwent HTC in a 300 mL Parr reactor (Moline, IL), at 260°C for 30 min. Literature reveals 260 °C being an ideal ratio for HTC for production due to the fixed carbon uptake and high mass yield as described by Islam et al. [17].The procedure was obtained from the literature [18,19]. Dried hydrochar was then mixed with MR and stirred, creating a homogenous sample. The following ratios were investigated: 50:50, 25:75, 10:90, and 5:95 (MR: hydrochar, dry basis). The mixture was then combined with potassium hydroxide (at a 4:1 ratio, potassium hydroxide: composite) and 25 mL of deionized water followed by prior study [20]. For example, 0.50 g of hydrochar were physically mixed with 0.50 g of MR, before being added to a $1.80 * 10^{-3}$ molar solution of KOH. After all the water had evaporated, activation was performed for 2 hours at 800 °C, an optimized activation temperature obtained from literature, under inert conditions [21]. Finally, the composites were then washed using 2 N HCl. This method allowed for the extraction of the potassium ions from the composite due to their attraction to the HCl, leaving pores in the sample [18]. This was done for all samples which were labeled according to their respective compositions with a "M" and an "H" before each respective ratio. Samples were labeled as follows: H5-M95, H10-M90, H25-M75, and H50:M50. The controls were labeled "MR" and "H260" after their respective base components of Martian regolith and hydrochar, respectively.

2.3. Product characterization

Using a Micrometrics HPVA II (Norcross, GA), the Braeuer, Emmett, and Teller (BET) surface area, the pore volume, and the pore size, of the samples, were obtained. A detailed description of the method employed can be found in the literature [22]. A brief explanation incorporates the measure of the adsorption of ultra-high purity nitrogen gas (N_2) between the given pressure values of $8 * 10^{-3}$ and 0.99 mPa. Liquid nitrogen was employed to keep a constant temperature of about 77 K. The data was processed through the Microactive software. This entailed the data, obtained via the utilization of relative pressure (P/P_o), which lay between the given values of 0.05 and 0.35. The same software was utilized for the micropore volume as well as the pore size distribution. This has an associated mechanical error of about 1 %.

The carbon, hydrogen, nitrogen, and sulfur content present in the samples were measured utilizing CHNS analysis (FLASH EA 1112 Series, Thermo Scientific, Grand Island, NY, USA). This had an associated mechanical error of 0.64, 0.16, and 0.11, respectively. Samples were prepared by measuring out a base ratio of 8–10 mg of vanadium oxide to 2–3 mg of sample. In order to provide a proper calibration, the method above was followed using vanadium oxide, 8–10 mg, and 2–3 mg of 5-tert-butyl-benzoxazol-2-yl thiophene (BBOT).

Thermogravimetric analysis TGA 4000 (PerkinElmer) was used to determine the thermal stability. This had a temperature error of about 1 °C. A sample of 5–15 mg was heated at a rate of 20°C /min from room temperature to 105°C under a 20 mL/min nitrogen purse. The temperature was held for 10 minutes and then heated from 105°C to 900°C at a rate of 50 °C/min. Once again, the temperature was held at 900°C for 5 minutes before being cooled to 575°C. The temperature was held for 10 minutes. The crystal structures of the samples were observed through X-ray diffraction (XRD) at a current of 10 MA. The data was collected on a spread of 2θ data points of 5 −80°. This had an approximate mechanical error of 0.01–0.02, 2θ. This was accomplished using a Bruker AXS X-ray diffraction system (model D2 Phaser SSD160) (Karlsruhe, Germany) under atmospheric pressure [20].

To physically observe the porosity of the composites, a JEOL JSM 6380LV Scanning Electron Microscope (SEM) (Tokyo, Japan) was utilized. The following parameters were utilized: a voltage range of 5–15 kV, a spot size of 40–60, and a magnification of 1000–4000. A Denton Vacuum Desk III (Moorestown, NJ) provided a layer of sputtered gold to improve the electroconductivity of the sample, allowing a substantial analysis to be completed. To obtain an idea of the composition of the composites, an EDX analyzer (Octane plus, EDAX, USA) was employed along with a voltage of 20 kV.

The composites underwent Fourier transform infrared radiation (FTIR) to identify the functional groups. Thermo Scientific Attenuated Total Reflector (ATR) FTIR (Model: Nicolet iS5, Madison, WI) was used. A background measurement was taken before each run using an accumulation of 64 scans per second over a range of wavelengths from (500–4000 cm^{-1}). This also utilized a resolution of 16 cm^{-1} in order to provide the highest resolution. This had an associated mechanical error of about 1 cm^{-1}. The samples were run under the same conditions as the background measurement.

Point of zero charge experiment was performed to observe the predisposed nature of the surface of the samples. This was done as best described by the literature [23]. To briefly summarize, in the "pH drift method," a fixed amount of base solute, KNO_3, and a fixed amount of

sample, was placed into 6 flasks and then adjusted to a pH of 2, 4, 6, 8, 10, and 12 respectively. This was then mixed for 24 hours at a fixed rate of 240 rpm.

2.4. Water retention and water holding capacity

In this study, water retention was observed by comparing the loss of weight in a composite, up to 105 °C, before and after total saturation. Literature has shown that TGA is an excellent method in which to observe the quantity of water in a sample, based on the difference of weight at a given temperature [24]. To start, about 0.12 g of composite were soaked in 40 mL of deionized (DI) water for 24 hours to ensure total saturation. After 24 hours, the DI water was removed via vacuum filtration, and 5–7 mg of the sample was analyzed via TGA to obtain an initial water content (W_i, %). Samples were allowed to dry for 24 hours at room temp, under atmospheric pressure before an additional 5–7 mg of sample was analyzed via TGA to obtain a final water content (W_f, %). The water saturation was then observed by taking the difference of the final and initial water content (Eq. 1).

$$\text{Water Retention} = W_f(\%) - W_i(\%) \tag{1}$$

In addition to the water retention, the water holding capacity (WHC) was also measured. WHC is defined as the ability of a substance to hold water against the force of gravity [25,26]. The method utilized was found in accordance with the literature [27]. In short, the WHC was found to be equivalent to the quotient of the difference of initial weight (W_0) and change of weight (ΔW) over the initial weight (Eq. 2). The initial weight was observed to be equivalent to one hundred times the initial water content of the sample (V_0) over the sum of the initial water content and the initial dry mass of the sample (D_0) (Eq. 3). The change of weight was found to be equivalent to one hundred times the difference in water content of the sample (ΔV_0) over the sum of the initial water content and the initial dry mass of the sample (Eq. 4).

$$\text{WHC} = \frac{W_0 - \Delta W}{W_0} \times 100\% \tag{2}$$

$$W_0 = \frac{V_0}{V_0 + D_0} \times 100\% \tag{3}$$

$$\Delta W = \frac{\Delta V_0}{V_0 + D_0} \times 100\% \tag{4}$$

3. Results and discussion

3.1. Surface morphology of co-activated Martian regolith with hydrochar

To elucidate the surface porosity evolution upon chemical activation of various MR- hydrochar mixtures, the surface porosity was quantified by characterizing BET-specific surface area (SSA), total pore volume (TPV), and micropore volume (MPV), as illustrated in Fig. 1. As observed in Fig. 1, with the increase of hydrochar constituent in the mixture, from 5 % to 50 %, there was almost three folds increase in BET SSA from 68.70 m^2/g to 265.40 m^2/g, whereas TPV and MPV increased by 84.4 % and 100 % respectively. This can be accounted for by an increased proportion of hydrochar in the mixture containing MR, before chemical activation, resulting in composites with enhanced surface porosity upon chemical activation. Conversely, decreased MR content in the mixture resulted in an enhanced pore formation as MR is an inorganic precursor, on which an activation agent has little to no effect on transforming it into a porous matrix upon activation [28,29]. Moreover, from the physicochemical characterization, it can be observed that MR has a carbon content of less than 1 %, as seen in Table 1, in which to exfoliate using KOH, in an attempt to create porosity through impregnation. Impregnation of hydrochar, with KOH, is known for its ablitiy to create high SSA [30]. Research have also reported that with an increased carbon content in the precursor from 48.70 % to 58.40 %, upon subsequent analogous KOH activation technique, the porosity development was substantially observed to increase from 1.24 cm^3/g to 1.56 cm^3/g respectivly, which can be accounted for by the optimized HTC aromatization and dehydration reaction rate [31].

To determine the amount of carbon, nitrogen, hydrogen, sulfur, and oxygen existing within the co-activated MR, CHNS results were examined and reported in Table 1. It was observed that MR contained less than 0.82, 0.57, and 0.31 wt% of carbon, nitrogen, and hydrogen, respectively. As also shown in Table 1, the hydrochar contained a wt% composition of 59.80, 0.85, and 4.58 % of carbon, nitrogen, and hydrogen, respectively, which follow the values discussed by Garlapalli et al. [32]. With increasing amounts of hydrochar, from 5 % to 50 %, the composite compositions of carbon, nitrogen, and hydrogen increased by 211.40 %, 20.30 %, and 396.6 %, respectively. It was also observed that the amount of oxygen, in the composites, slightly decreased with the addition of hydrochar from 73 wt% to 66.80 %. MR has a high metal oxide content and thus contributes a large portion of oxygen to the CHNS composition, but has a low organic matter content [6]. In contrast, hydrochar has an enriched carbon content due to the organic

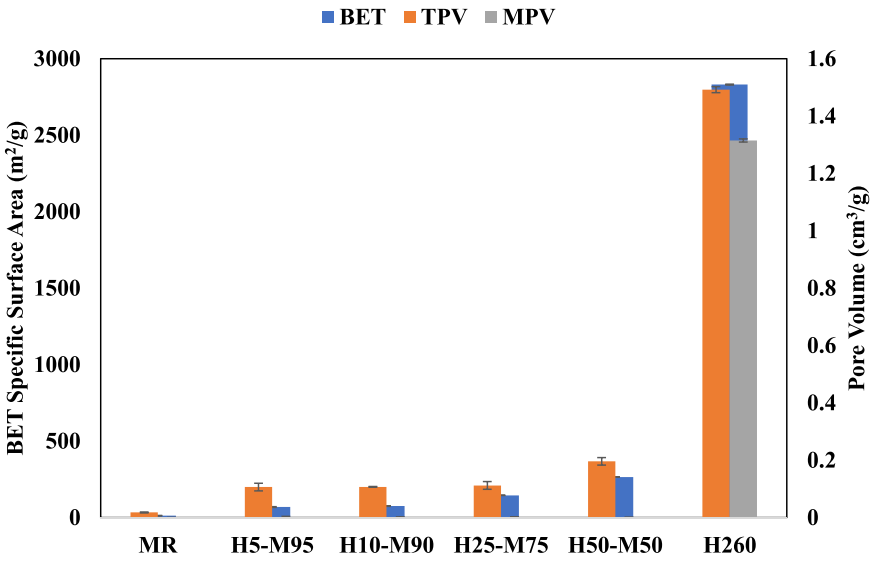

Fig. 1. Surface porosity characterization of co-activated Martian regolith with hydrochar.

Table 1
Physical and chemical characterizations of co-activated Martian regolith with hydrochar at different ratios.

Sample	Surface pH	pH_{PZC}	Carbon (%)	Nitrogen (%)	Hydrogen (%)	Sulfur (%)	Oxygen (%)	Ash (%)
MR	6.98	6.80	0.82 ± 0.07	0.58 ± 0.29	0.03 ± 0.03	0 ± 0.12	93.50 ± 0.06	95.20
H5-M95	9.38	9.71	1.20 ± 0.64	0.57 ± 0.27	1.50 ± 0.84	0 ± 0	72.90 ± 1.60	76.30
H10-M90	10.11	10.65	2.10 ± 0.27	0.69 ± 0.34	2.10 ± 0.17	0 ± 0	73.60 ± 0.79	78.60
H25-M75	9.96	10.30	1 ± 0.27	0.66 ± 0.31	1.60 ± 0.19	0 ± 0.07	82.40 ± 0.25	85.60
H50-M50	9.26	9.55	5.80 ± 1.30	0.87 ± 0.41	0.81 ± 0.48	0 ± 0.08	66.80 ± 1.8	74.30
H260	4.63	3.70	59.80 ± 1.50	0.85 ± 0.02	4.60 ± 0.06	0 ± 0	0 ± 1.50	10.90

nature of its precursor material, LP, as well as due to the aromaticity process during the production and activation [31,33].

3.2. Chemical and physical properties of co-activated Martian regolith with hydrochar

To analyze the thermal stability of the composites, TGA results were displayed in Fig. 2. As observed in Fig. 2, co-activated MRs exhibit a thermally stable curve, with an increasing amounts of MR. These results differ greatly from the control hydrochar, which degrades and looses an approximate 45 % more weight then that of the samples. With the decrease of hydrochar, from 50 % to 5 %, there was an increase in the amount of non-combustible material, ash, from 74.20 % to 76.30 %. This observation of high amounts of non-combustible material is indicated towards the amount of inorganic material in MR, as explained later.

To better evaluate the crystallinity and nature of the inorganic compounds present in the co-activated MR, XRD results were analyzed and plotted in Fig. 3. Cannon *et al.* reported the composition of MR to be 43.20 % silicon oxide, 1.20 % titanium oxide, 9.40 % aluminum oxide, 0.50 chromium oxide, 19.20 % iron oxides, 0.40 % manganese oxide, 8.70 % magnesium oxide, 7.30 % calcium oxide, 2.70 % sodium oxide, 0.50 % potassium oxide, 1 % phosphoric oxide, 5.50 % sulfur trioxide, and a balance of chlorine [6]. Aluminum and silicon oxides were both prevalent in consideration of the elemental composition [28,34]. This appears in the forms of Ferroan forsterite ($Mg_{1.2}Fe_{0.8}SiO_4$), Forsterite ($Mg_{1.8}Fe_{0.2}SiO_4$), and Plagiclase ($Ca_{0.88}Na_{0.12}Al_{1.77}Si_{2.23}O_8$) [29,35]. Ferroan forsterite shows its prevalence at the 2 theta (2θ) values of 20°, 26°, 42°, and 60–62° [36]. Forsterite follows a similar trend. Plagioclase shows relevance in the 2θ values of 25.5° and 32–33° [37]. Iron oxides were noted to be prominent in the form of Hematite (27°, 38°, and 58°),

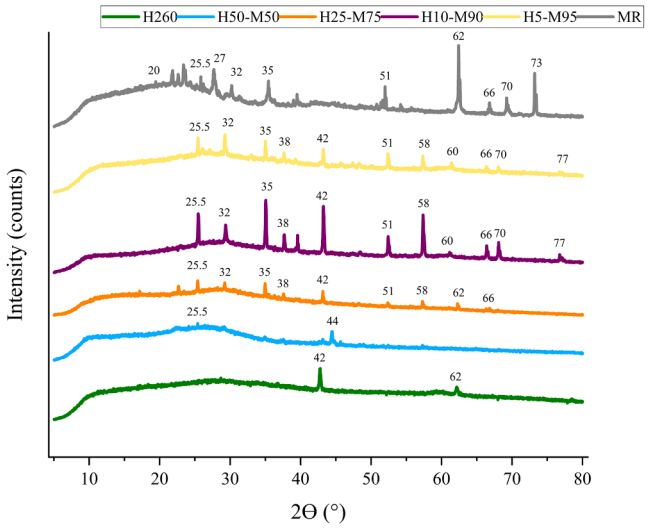

Fig. 3. Crystallinity of co-activated Martian regolith with hydrochar.

Maghemite (35°), and elemental iron (52°)[36,38]. Hydrochar was noted to contain a single silicon oxide peak at about 42° and 62° [39]. It was observed that as the amount of hydrochar increased from 10 % to 50 %, the intensity of crystalline structures decreased significantly due to the increase of noncrystalline organic structures.

To better observe the surface functionality of the co-activated MR, the FTIR data was quantified and displayed in Fig. 4. MR containing samples at a broad peak range between 3304 cm^{-1} and 3418 cm^{-1} were observed to be ascribed to O-H bonds. At about 1650 cm^{-1}, samples

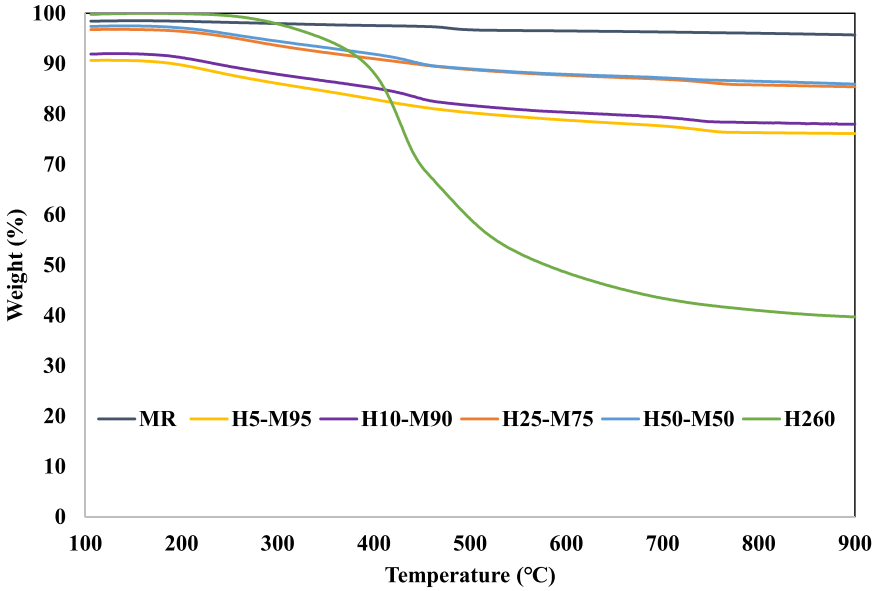

Fig. 2. Thermogram of co-activated Martian regolith with hydrochar.

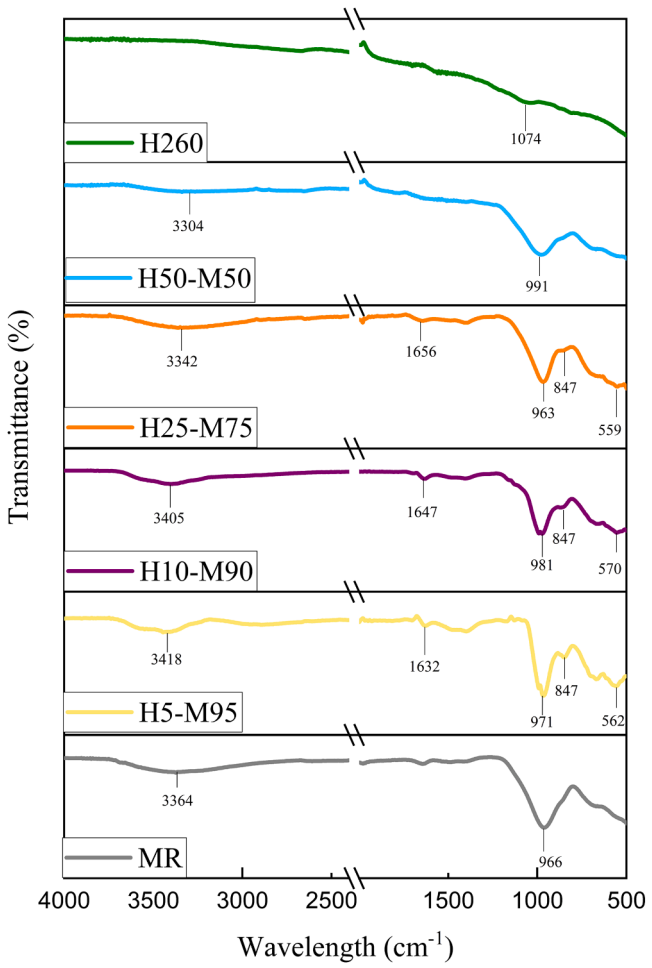

Fig. 4. FTIR analysis of co-activated Martian regolith with hydrochar.

with hydrochar defiant compositions were observed to display C═O bonds in the form of amide I [40]. Hydrochar showed a conformation of C-H angular deformation at 1074 cm^{-1}, linked to the aromatic structure contained in the sample [41,42]. As hydrochar content decreases in composition, samples show the presence of Si-O-Si which can best be described by the literature to be reflected at about 987 cm^{-1} [43,44]. Hydrochar-deficient composites of less than 50 % hydrochar showed conformations of Al-OH-Fe at about 847 cm^{-1} when a strong O-H bond was prevalent [43,45]. Finally, it was observed that all MR-containing products showed peaks at about 570 cm^{-1}, attributed to S-S and C-S bonds [40,46].

In addition to characterizing the surface functionality of the co-activated MR, the effect on the pH was desired by computing the surface pH and the point of zero charge, as quantified in Table 1. It was observed that with increasing amounts of hydrochar, from 5 % to 50 %, the surface pH was measured to be 9.38 and 9.26, respectively. This value increased by 3.40 % and 3.04 % respectively, indicating the formation of basic functional groups on the surface of the co-activated MR [23,47].

In order to further observe the surface functionality of the co-activated MR, the point of zero charge and surface pH was obtained in Table 1. It was observed that the MR had a surface charge of about 7 and a point of zero charge of about 6.80. As described by Fiol et al., the surface pH and point of zero charge reveal the affinity, of the substance, for interaction with ionized bonding sites, pointing towards MR having an affinity for the sorption of anions [48]. To the author's knowledge, no previous studies on the surface pH or point of zero charge of MR, have been reported. Hydrochar had a surface charge and point of zero charge of about 4.60 and 3.70, respectively, also indicating a positive affinity for the sorption of anions. The results are in agreement with the literature values of about 4.10 and 3.70 respectively [23]. After activation, it was observed that the co-activated MRs displayed that they had a surface pH of about 9.40, 10.10, 10, and 9.60 with increasing amounts of hydrochar. When paired affinity for the sorption of cations due to the point of zero charge being greater than that of the surface pH [49].

3.3. Water retention and water holding capacity of co-activated Martian regolith

With the goal of extraterrestrial exploration and advancing life on Mars, the ability to prevent the loss of water from Martian regolith has been pivotal. It can be observed in Fig. 5 that as the amount of hydrochar increased from 5 % to 50 % in composition, the amount of water lost, after 24 hours, increased by 20 wt%. This can be attributed to the high silicon, and other metal oxide contents in the composite samples [50,51]. Amiinu *et al.* discussed the impact of silicon oxide on water, utilizing surface adsorption as the driving mechanism [52]. In short, the surface silicon bonds with a hydroxide group from the water, which then loosely bonds to another silicon molecule. This forms a solid structure that has a hydrophilic shell and a hydrophobic interior [51–53]. This is applicable when consideration of the large quantities of ice observed on the surface of Mars [54].

Although this allows insight into how the co-activated MR will act over 24 hours, the water holding capacity (WHC) was found to observe the rate of total saturation possible, giving further insight into water retention capabilities. The WHC of MR and hydrochar were observed to be about 30 % and 50 % in value, as depicted in Fig. 6. With the addition of hydrochar, from 5 % to 50 %, it was observed that the WHC decreased from 96.20 % to 80.92 % respectively, as also observed in Fig. 6. Although hydrochar is an effective method to increase the surface area, demonstrating an increased surface area of the composites by 386.60 %, from 5 % to 50 % of hydrochar constituent in composites, the natural hydrophobic tendencies of hydrochar, can hinder the WHC [55,56]. Therefore, deriving MR- hydrochar composites could be a promising route of imparting moisture in Mars regolith.

4. Conclusions

The objective of this study was to co-activate Martian regolith (MR) with loblolly pine-derived hydrochar to innovate the porous carbon materials that can lay the foundation for future space applications in advancing agriculture and hence life on Mars. A variety of ratios of hydrochar to MR were extensively investigated and the primary findings successfully demonstrated to improve surface characteristics, including increased surface area and pore volume 265.40 m^2/g and 1.56 cm^3/g as

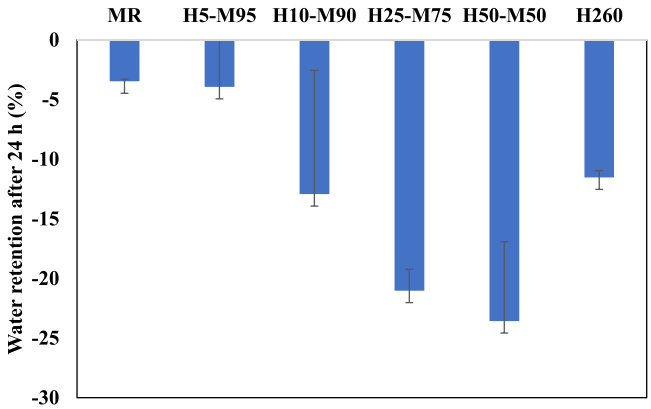

Fig. 5. Water retention of co-activated Martian regolith and hydrochar after 24 h.

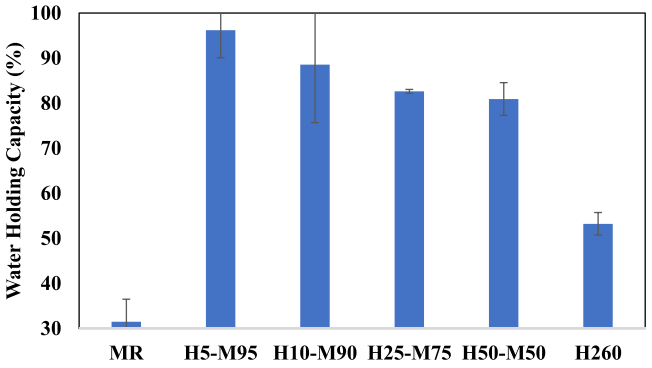

Fig. 6. Water holding capacity of co-activated Martian regolith with hydrochar.

well as an increased carbon content of 211.40 % more than that of MR, in the case of 50 % hydrochar composition. Furthermore, the capacity to retain water in MR was substantially improved via co-activation of MR as it recorded favorable trends of low water loss, as low as 4 %, and minimal water loss, of less than 1 %. Therefore, it was effectively concluded that with the addition of hydrochar, the properties of MR could be favorably enhanced with the optimal ratio, in this study, containing 50 % hydrochar due to its high surface area, porosity, and carbon content, as well as a high water retention capacity and compatible water holding capacity.

CRediT authorship contribution statement

Reza Toufiq: Writing – review & editing, Supervision, Resources, Project administration, Investigation, Funding acquisition, Conceptualization. **Sultana Al Ibtida:** Methodology, Investigation, Formal analysis, Data curation, Conceptualization. **Cheatham Robert W.:** Writing – original draft, Formal analysis, Data curation, Conceptualization.

Declaration of Competing Interest

The authors declare no competing interests.

Acknowledgements

The authors express thanks to Dr. Tatiana Karpova, undergraduate students Josh Calhoun, and Russell Smith at Florida Institute of Technology.

Ethics approval and consent to participate

Not applicable.

Consent for publication

Robert Cheatham, Al Ibtida Sultana, and Toufiq Reza consent to the paper being published.

Data Availability

Data will be made available on request.

References

[1] S. Jaber, Op-ed Materials that could bring life to Mars, in Space News vol. 2024, ed. Space News, 2020.
[2] R.M. Candanosa. "Growing Green on the Red Planet." https://www.acs.org/education/resources/highschool/chemmatters/past-issues/2016-2017/april-2017/growing-green-on-the-red-planet.html (accessed 11.20.23.
[3] A. Robinson. "What Would It Take to Feed One Million People on Mars?." ⟨https://modernfarmer.com/2019/09/what-would-it-take-to-feed-one-million-people-on-mars/⟩ (accessed 11.20, 2023).
[4] L.G. Duri, et al., Mars regolith simulant ameliorated by compost as in situ cultivation substrate improves lettuce growth and nutritional aspects, Plants 9 (5) (2020) 628. ⟨https://www.mdpi.com/2223-7747/9/5/628⟩ ([Online]. Available).
[5] G.W.W. Wamelink, J.Y. Frissel, W.H.J. Krijnen, M.R. Verwoert, Crop growth and viability of seeds on Mars and Moon soil simulants, Open Agric. 4 (1) (2019) 509–516, https://doi.org/10.1515/opag-2019-0051.
[6] K.M. Cannon, D.T. Britt, T.M. Smith, R.F. Fritsche, D. Batcheldor, Mars global simulant MGS-1: a rocknest-based open standard for basaltic martian regolith simulants, 2019/01/01/, Icarus 317 (2019) 470–478, https://doi.org/10.1016/j.icarus.2018.08.019.
[7] A. Robinson. "Study Suggests Farmers Could Grow Crops on Mars." ⟨https://modernfarmer.com/2019/10/study-suggests-farmers-could-grow-crops-on-mars/⟩ (accessed 11.20, 2023).
[8] J. Jänchen, et al., Water retention of selected microorganisms and Martian soil simulants under close to Martian environmental conditions, 2014/08/01/, Planet. Space Sci. 98 (2014) 163–168, https://doi.org/10.1016/j.pss.2013.06.011.
[9] A.G. Caporale, et al., Can Lunar and Martian soils support food plant production? Effects of horse/swine monogastric manure fertilisation on regolith simulants enzymatic activity, nutrient bioavailability, and lettuce growth, Plants 11 (23) (2022) 2022, https://doi.org/10.3390/plants11233345.
[10] S. Bikbulatova, A. Tahmasebi, Z. Zhang, S.K. Rish, J. Yu, Understanding water retention behavior and mechanism in bio-char, 2018/01/01/, Fuel Process. Technol. 169 (2018) 101–111, https://doi.org/10.1016/j.fuproc.2017.09.025.
[11] R.A. Brown, A.K. Kercher, T.H. Nguyen, D.C. Nagle, W.P. Ball, Production and characterization of synthetic wood chars for use as surrogates for natural sorbents, Org. Geochem. 37 (3) (2006) 321–333.
[12] Z. Tan, C.S. Lin, X. Ji, T.J. Rainey, Returning biochar to fields: A review, Appl. Soil Ecol. 116 (2017) 1–11.
[13] J. Ulyett, R. Sakrabani, M. Kibblewhite, M. Hann, Impact of biochar addition on water retention, nitrification and carbon dioxide evolution from two sandy loam soils, Eur. J. Soil Sci. 65 (1) (2014) 96–104.
[14] T. Garbowski, D. Bar-Michalczyk, S. Charazińska, B. Grabowska-Polanowska, A. Kowalczyk, P. Lochyński, An overview of natural soil amendments in agriculture, 2023/01/01/, Soil Tillage Res. 225 (2023) 105462, https://doi.org/10.1016/j.still.2022.105462.
[15] T. Quaid, V. Ghalandari, and T. Reza, Effect of Synthesis Process, Synthesis Temperature, and Reaction Time on Chemical, Morphological, and Quantum Properties of Carbon Dots Derived from Loblolly Pine, Biomass, vol. 2, no. 4, pp. 250-263doi: 10.3390/biomass2040017.
[16] Q. Wu, L. Huang, S. Yu, S. Liu, C. Xie, A.J. Ragauskas, Structural elucidation of hydro-products from hydrothermal carbonization of loblolly pine at different temperatures using NMR techniques, 2017/08/15/, Energy 133 (2017) 171–178, https://doi.org/10.1016/j.energy.2017.05.040.
[17] M.T. Islam, N. Saha, S. Hernandez, J. Klinger, M.T. Reza, Integration of air classification and hydrothermal carbonization to enhance energy recovery of corn stover, Energies 14 (5) (2021) 1397. ⟨https://www.mdpi.com/1996-1073/14/5/1397⟩ ([Online]. Available).
[18] M.T. Reza, J.G. Lynam, M.H. Uddin, C.J. Coronella, Hydrothermal carbonization: fate of inorganics, 2013/02/01/, Biomass-. Bioenergy 49 (2013) 86–94, https://doi.org/10.1016/j.biombioe.2012.12.004.
[19] G.-g Huang, Y.-f Liu, X.-x Wu, J.-j Cai, Activated carbons prepared by the KOH activation of a hydrochar from garlic peel and their CO2 adsorption performance, 2019/06/01/, N. Carbon Mater. 34 (3) (2019) 247–257, https://doi.org/10.1016/S1872-5805(19)60014-4.
[20] A.I. Sultana, R.W. Cheatham, M.T. Reza, Deep eutectic solvent pretreatment alters surface morphology and functionality of activated hydrochar resulting in enhanced carbon dioxide capture, 2023, J. CO2 Util. 68 (2023) 102350, https://doi.org/10.1016/j.jcou.2022.102350.
[21] S.Hui Tang, A. Zaini Muhammad Abbas, Potassium hydroxide activation of activated carbon: a commentary, (in En), 2015/10/31/, Carbon Lett. 16 (4) (2015) 275–280, https://doi.org/10.5714/CL.2015.16.4.275.
[22] C. Wedler, R. Span, Micropore analysis of biomass chars by co2 adsorption: comparison of different analysis methods, 2021/05/20/, Energy Fuels 35 (10) (2021) 8799–8806, https://doi.org/10.1021/acs.energyfuels.1c00280.
[23] N. Saha, A. Saba, M.T. Reza, Effect of hydrothermal carbonization temperature on pH, dissociation constants, and acidic functional groups on hydrochar from cellulose and wood, 2019, J. Anal. Appl. Pyrolysis 137 (2019) 138–145, https://doi.org/10.1016/j.jaap.2018.11.018.
[24] Y. Meng, et al., Super-swelling lignin-based biopolymer hydrogels for soil water retention from paper industry waste, 2019/08/15/, Int. J. Biol. Macromol. 135 (2019) 815–820, https://doi.org/10.1016/j.ijbiomac.2019.05.195.
[25] D. Koops, Know Your Water Holding Capacity." [Online]. Available: ⟨https://www.cropquest.com/know-your-water-holding-capacity/⟩.
[26] E.M.C.C. Batista, et al., Effect of surface and porosity of biochar on water holding capacity aiming indirectly at preservation of the Amazon biome, 2018/07/16, Sci. Rep. 8 (1) (2018) 10677, https://doi.org/10.1038/s41598-018-28794-z.
[27] Hettich. "Water Holding Capacity (WHC) and Cook Loss Determination of Fish Muscle." ⟨https://www.hettweb.com/applications/water-holding-capacity-and-cook-loss-in-fish-muscle/⟩ (accessed 11/20/2023, 2023).
[28] S. K, P. Sinha, P. Chaunsali, Development of waterless extra-terrestrial concrete using Martian regolith, 2023/07/24/, Adv. Space Res. (2023), https://doi.org/10.1016/j.asr.2023.07.036.

[29] D. Karl, et al., Clay in situ resource utilization with Mars global simulant slurries for additive manufacturing and traditional shaping of unfired green bodies, 2020/09/01/, Acta Astronaut. 174 (2020) 241–253, https://doi.org/10.1016/j.actaastro.2020.04.064.
[30] K.K.H. Choy, J.P. Barford, G. McKay, Production of activated carbon from bamboo scaffolding waste—process design, evaluation and sensitivity analysis, 2005/05/01/, Chem. Eng. J. 109 (1) (2005) 147–165, https://doi.org/10.1016/j.cej.2005.02.030.
[31] A.I. Sultana, M.T. Reza, Investigation of hydrothermal carbonization and chemical activation process conditions on hydrogen storage in loblolly pine-derived superactivated hydrochars, 2022/07/22/, Int. J. Hydrog. Energy 47 (62) (2022) 26422–26434, https://doi.org/10.1016/j.ijhydene.2022.04.128.
[32] R.K. Garlapalli, B. Wirth, M.T. Reza, Pyrolysis of hydrochar from digestate: Effect of hydrothermal carbonization and pyrolysis temperatures on pyrochar formation, 2016/11/01/, Bioresour. Technol. 220 (2016) 168–174, https://doi.org/10.1016/j.biortech.2016.08.071.
[33] R. Pedicini, S. Maisano, V. Chiodo, G. Conte, A. Policicchio, R.G. Agostino, Posidonia oceanica and Wood chips activated carbon as interesting materials for hydrogen storage, 2020/05/18/, Int. J. Hydrog. Energy 45 (27) (2020) 14038–14047, https://doi.org/10.1016/j.ijhydene.2020.03.130.
[34] L.E. Fackrell, P.A. Schroeder, A. Thompson, K. Stockstill-Cahill, C.A. Hibbitts, Development of martian regolith and bedrock simulants: potential and limitations of martian regolith as an in-situ resource, 2021/01/15/, Icarus 354 (2021) 114055, https://doi.org/10.1016/j.icarus.2020.114055.
[35] C.N. Achilles, et al., Mineralogy of an active eolian sediment from the Namib dune, Gale crater, Mars, 2017/11/01, J. Geophys. Res.: Planets 122 (11) (2017) 2344–2361, https://doi.org/10.1002/2017JE005262.
[36] D.L. Bish, et al., X-ray diffraction results from mars science laboratory: mineralogy of rocknest at gale crater, 2013/09/27/, Science 341 (6153) (2013) 1238932, https://doi.org/10.1126/science.1238932.
[37] D. Karl, et al., Sintering of ceramics for clay in situ resource utilization on Mars, 2020/09/01/, Open Ceram. 3 (2020) 100008, https://doi.org/10.1016/j.oceram.2020.100008.
[38] L. Karacasulu, D. Karl, A. Gurlo, C. Vakifahmetoglu, Cold sintering as a promising ISRU technique: a case study of Mars regolith simulant, 2023/01/01/, Icarus 389 (2023) 115270, https://doi.org/10.1016/j.icarus.2022.115270.
[39] S. Sukarni, et al., Combustion of microalgae Nannochloropsis oculata biomass: cellular macromolecular and mineralogical content changes during thermal decomposition, Songklanakarin J. Sci. Technol. 40 (6) (2018).
[40] J. Coates, Interpretation of Infrared Spectra, A Practical Approach, in Encyclopedia of Analytical Chemistry.
[41] S. El Ichi, et al., Chitosan improves stability of carbon nanotube biocathodes for glucose biofuel cells, 10.1039/C4CC04862H, Chem. Commun. 50 (93) (2014) 14535–14538, https://doi.org/10.1039/C4CC04862H.
[42] S. Saha, M.T. Islam, J. Calhoun, T. Reza, Effect of hydrothermal carbonization on fuel and combustion properties of shrimp shell waste, Energies 16 (14) (2023) 2023, https://doi.org/10.3390/en16145534.
[43] W. Yan, D. Liu, D. Tan, P. Yuan, M. Chen, FTIR spectroscopy study of the structure changes of palygorskite under heating, 2012/11/01/, Spectrochim. Acta Part A: Mol. Biomol. Spectrosc. 97 (2012) 1052–1057, https://doi.org/10.1016/j.saa.2012.07.085.
[44] D.A. McKeown, J.E. Post, E.S. Etz, Vibrational analysis of palygorskite and sepiolite, Clays Clay Miner. 50 (5) (2002) 667–680, https://doi.org/10.1346/000986002320679549.
[45] R.L. Frost, G.A. Cash, J.T. Kloprogge, 'Rocky Mountain leather', sepiolite and attapulgite - An infrared emission spectroscopic study, Vib. Spectrosc. 16 (2) (1998) 173–184, https://doi.org/10.1016/S0924-2031(98)00014-9.
[46] S. Kannan, Y. Gariepy, G.S.V. Raghavan, Optimization and characterization of hydrochar derived from shrimp waste, 2017/04/20, Energy Fuels 31 (4) (2017) 4068–4077, https://doi.org/10.1021/acs.energyfuels.7b00093.
[47] N. Saha, M. Volpe, L. Fiori, R. Volpe, A. Messineo, M.T. Reza, Cationic dye adsorption on hydrochars of winery and citrus juice industries residues: performance, mechanism, and thermodynamics, Energies 13 (18) (2020) 2020, https://doi.org/10.3390/en13184686.
[48] N. Fiol, I. Villaescusa, Determination of sorbent point zero charge: usefulness in sorption studies, 2009/02/01, Environ. Chem. Lett. 7 (1) (2009) 79–84, https://doi.org/10.1007/s10311-008-0139-0.
[49] P.M. Mosur, Y.M. Chernoberezhskii, A.V. Lorentsson, Electrosurface properties of microcrystalline cellulose dispersions in aqueous solutions of aluminum chloride, nitrate, and sulfate, 2008/08/01, Colloid J. 70 (4) (2008) 462–465, https://doi.org/10.1134/S1061933X08040091.
[50] S.K. Sah, K.R. Reddy, and J. Li, Silicon Enhances Plant Vegetative Growth and Soil Water Retention of Soybean (Glycine max) Plants under Water-Limiting Conditions, Plants, vol. 11, no. 13, doi: 10.3390/plants11131687.
[51] D. Blanco, O. Antikainen, H. Räikkönen, J. Yliruusi, A.M. Juppo, Effect of colloidal silicon dioxide and moisture on powder flow properties: Predicting in-process performance using image-based analysis, 2021/03/15/, Int. J. Pharm. 597 (2021) 120344, https://doi.org/10.1016/j.ijpharm.2021.120344.
[52] I. A, Y. Lin, H. Tang, M. Pan, and H. Zhang, Metal Oxides as Water Retention Materials For Low Humidity Proton Exchange Membrane Applications, 2013, pp. 81-108..
[53] D. Elahe, B. Hossein, Z. Pouya, Effect of oxide nanoparticles on soil water retention curve and soil tensile strength, 2023/08/01/, Pedosphere (2023), https://doi.org/10.1016/j.pedsph.2023.07.017.
[54] S.W. Squyres, M.H. Carr, Geomorphic evidence for the distribution of ground ice on mars, 1986/01/17, Science 231 (4735) (1986) 249–252, https://doi.org/10.1126/science.231.4735.249.
[55] J. Fan, et al., Effects of hydrophobic coating on properties of hydrochar produced at different temperatures: specific surface area and oxygen-containing functional groups, 2022/11/01/, Bioresour. Technol. 363 (2022) 127971, https://doi.org/10.1016/j.biortech.2022.127971.
[56] Y. Pu, J.X. Wang, D. Wang, N.R. Foster, J.F. Chen, Subcritical water processing for nanopharmaceuticals (Review), Chem. Eng. Process. - Process. Intensif. 140 (2019) 36–42, https://doi.org/10.1016/j.cep.2019.04.013.